NASA TECHNICAL NOTE

NASA TN D-1966

NASA TN D-1966

STEADY-STATE CHARACTERISTICS OF A DIFFERENTIAL-PRESSURE SYSTEM FOR EVALUATING ANGLES OF ATTACK AND SIDESLIP OF THE RANGER IV VEHICLE

by E. Carson Yates, Jr., and Annie G. Fox
Langley Research Center
Langley Station, Hampton, Va.

NATIONAL AERONAUTICS AND SPACE ADMINISTRATION • WASHINGTON, D. C. • NOVEMBER 1963

TECHNICAL NOTE D-1966

STEADY-STATE CHARACTERISTICS OF A DIFFERENTIAL-PRESSURE SYSTEM FOR EVALUATING ANGLES OF ATTACK AND SIDESLIP OF THE RANGER IV VEHICLE

By E. Carson Yates, Jr., and Annie G. Fox

Langley Research Center
Langley Station, Hampton, Va.

NATIONAL AERONAUTICS AND SPACE ADMINISTRATION

NATIONAL AERONAUTICS AND SPACE ADMINISTRATION

TECHNICAL NOTE D-1966

STEADY-STATE CHARACTERISTICS OF A DIFFERENTIAL-PRESSURE SYSTEM FOR EVALUATING ANGLES OF ATTACK AND SIDESLIP OF THE RANGER IV VEHICLE

By E. Carson Yates, Jr., and Annie G. Fox

SUMMARY

An investigation has been conducted in the Langley 26-inch transonic blowdown tunnel at Mach numbers from 0.58 to 1.31 to examine some of the characteristics of a differential-pressure system used to measure flow angles over the hemisphere-cone nose of the Ranger IV vehicle. The differential pressures were measured between two orifices located in the pitch plane at 45° off the center line of the hemisphere nose. The effects of variations in Mach number, Reynolds number, pitch angle, and combined pitch and yaw angles on the differential-pressure characteristics were studied.

The results indicated that, for a given total pressure and Mach number, the differential pressure varied linearly with pitch angle and was unaffected by variations in Reynolds number and yaw angle within the range of this investigation. As Mach number increased above 1, a decreasing effect of afterbody shape was shown.

INTRODUCTION

A method which has been used successfully for determining angles of attack or angles of sideslip for missiles and space vehicles is based on measurements of surface pressure differences between two or more selected points near the vehicle nose. Quantitative knowledge of the relations between such pressure differences and the associated flow angularities permit an interpretation of flight-measured pressure data in terms of the flow angles encountered by the vehicle. In comparison with the vane or angle-head type of flow-angle-measuring system, the differential-pressure system offers several advantages. (See refs. 1 and 2, for example.) The differential-pressure system is simple, rugged, heat resistant, and adds no drag nor significant structural loads to the vehicle. The angle-head system, on the other hand, is generally heavier and may require multiple installations. Both the angle-head system and the differential-pressure system, however, are influenced by the vehicle flow field.

This report examines some of the more important characteristics of the differential-pressure system used on the hemisphere-cone nose shroud of the Ranger IV vehicle. (See fig. 1.) Differential pressures were measured on a 0.04565-scale model of the nose of this vehicle (fig. 1) in the Langley 26-inch transonic blowdown tunnel at pitch angles from -10° to 10° and at Mach numbers from 0.58 to 1.31. Existing theoretical and experimental data (refs. 2 to 7, for example) on similar configurations were considered to provide adequate information for higher Mach numbers. The present experiments also indicate some effects of combined pitch and yaw angles and of variations in Reynolds number.

SYMBOLS

M	free-stream Mach number
Δp	(pressure at orifice 1) - (pressure at orifice 2) (See fig. 1.)
q	free-stream dynamic pressure
R	Reynolds number based on nose radius
θ	geometric pitch angle of model measured in meridian plane containing orifices 1 and 2
θ_s	angle between model axis and tunnel center line
ψ	geometric yaw angle of model measured in meridian plane perpendicular to that containing orifices 1 and 2
φ	roll angle of model measured about model axis of symmetry ($\varphi = 0$ when orifice 1 is above orifice 2 and both lie in a vertical plane that contains the tunnel center line)

MODEL

This investigation employed a 0.04565-scale machined aluminum model of the nose of the Ranger IV vehicle. (See figs. 1 and 2.) Only a small portion of the cylindrical second-stage Agena B vehicle was represented because on the basis of previous data from the Langley 8-foot transonic pressure tunnel, portions of the combined vehicle farther aft would be expected to have negligible effect on pressures on the hemispherical nose.

The nose of the ranger IV vehicle was fitted with five pressure-measuring orifices as shown in figure 1. One of these was on the vehicle center line, and the other four were located 45° off the center line (two in the pitch plane and two in the yaw plane). The center-line orifice (orifice 5 in fig. 1) was not installed on the model because measurements of total pressure on the model were not required in the present investigation. Furthermore, pressure measurements on the vehicle are not essential for the evaluation of dynamic pressures along

the flight path. Since the Ranger IV vehicle was a body of revolution, the relations between angle of attack (or pitch angle) and the pressure difference for orifices 1 and 2 should be the same as the relations between sideslip angle (or yaw angle) and the pressure difference for orifices 3 and 4. Hence, only orifices 1 and 2 were provided on the model. For reasons of practical fabrication, these orifices on the model (0.0135-inch diameter) were about five times as large as the size indicated by the model scale. The larger orifices, however, are not considered to affect the present results significantly because the variation of pressure across the orifice diameter should average out to approximately the true value for the orifice-center location. Pressure leads from these orifices were 0.040-inch inside-diameter aluminum tubing. With pressure leads of this size, the 0.0135-inch-diameter orifices should not contribute significantly to response lag when surface pressures are changed. (See ref. 8.) Although dynamic response was not studied in this investigation, a small lag in the pressure-measuring system was desirable in order to facilitate efficient use of the limited running time of the tunnel.

APPARATUS AND TESTS

The model was tested on a sting mount in the Langley 26-inch transonic blowdown tunnel which has a slotted, octagonal test section measuring approximately 26 inches across flats. (See refs. 9 and 10.) The two pressure leads from the model were attached to a differential-pressure transducer located in the sting. Transducers rated ±10, ±15, and ±25 pounds per square inch were used interchangeably depending on the pressure-range requirements anticipated for each test run. The pressure-response calibrations of these transducers were linear within the rated pressure ranges and were unaffected by absolute pressure level or by inverting the transducers.

The operating capabilities of the Langley 26-inch transonic blowdown tunnel permit Mach number and Reynolds number to be varied independently. For each test run of this investigation, the Mach number and the stagnation pressure were held essentially constant while the model was programed through an angle range from about $\theta_s = 10^\circ$ to about $\theta_s = -10^\circ$ in 2° increments. At all angles, the center of the hemispherical nose of the model remained approximately on the tunnel center line. Throughout each run the output of the differential-pressure transducer as well as indications of tunnel stagnation temperature and stagnation and static pressures were continuously recorded by an oscillograph. Some electrical smoothing of the transducer output was required to offset the effects of tunnel turbulence. It should be noted that since the tunnel temperature dropped continuously during each run, the Reynolds number increased to some extent (10 to 20 percent) during each run. Consequently, the Reynolds number values given herein are mean values for each run.

Most of the runs were made with $\varphi = 0^\circ$. However, some runs were made with the model inverted ($\varphi = 180^\circ$) in order to separate the effects of tunnel-flow angularity and of any model asymmetry that might exist. Several runs were also made with $\varphi = 45^\circ$, 135°, and 315° in order to determine the effects of combined pitch and yaw. If the model is rolled about its axis of symmetry ($\varphi \neq 0$), the

pitch angle θ measured in the meridian plane containing orifices 1 and 2 is related to the angle θ_s by

$$\tan \theta = \cos \varphi \tan \theta_s \tag{1}$$

and to the yaw angle ψ by

$$\tan \theta = \frac{\tan \psi}{\tan \varphi} \tag{2}$$

Thus, for the tests with $\varphi = 45^\circ$, 135°, and 315°,

$$|\theta| = |\psi|$$

and any effect of yaw should be most evident at the larger deflections θ_s.

No corrections have been applied to the present data for wall interference, flow angularity, or blockage. However, on the basis of repeatability checks, instrument accuracies, and calibrations, the following uncertainties are considered to exist in the present measurements:

M	±0.005
q, lb/sq in.	±0.2
Δp, lb/sq in.	±0.1
θ_s, deg	±0.08

RESULTS AND DISCUSSION

Relation of Differential Pressure to Geometric Pitch Angle

Figure 3 presents typical curves of $\frac{\Delta p}{q}$ as a function of the geometric pitch angle θ. These curves show that $\frac{\Delta p}{q}$ changes linearly with θ at least over the range of $-9^\circ \leq \theta \leq 9^\circ$. Within the limits of this investigation, linearity in this pitch-angle range was unaffected by varying Mach number, varying Reynolds number, or by inverting the model ($\varphi = 180^\circ$). A linear relation between $\frac{\Delta p}{q}$ and θ is characteristic for hemisphere-cylinders and hemisphere-cones provided the cone angle and the pitch angle are not too large. (See ref. 1, for example.) Within the θ range of the present experiments, it is therefore feasible to describe the differential-pressure characteristics in terms of the slope of the curves of $\frac{\Delta p}{q}$ plotted against θ, that is, in terms of $\frac{\partial\left(\frac{\Delta p}{q}\right)}{\partial \theta}$. The variation of this pressure index with Mach number is shown in figure 4.

The shape of this curve is typical for hemisphere-cones as is illustrated in figure 5 which shows the curve of figure 4 in relation to similar results for a hemisphere-cone with 10° half-angle obtained in the Langley 8-foot transonic pressure tunnel and for a hemisphere-cylinder.[1] As Mach number increases into the supersonic range, the three curves tend to converge, and thus indicate the reduced importance of afterbody shape at the higher Mach numbers. (See also ref. 3.) However, in comparison with the other two curves, the present results would require higher Mach numbers for complete convergence because of the larger cone half-angle (15°) of the Ranger vehicle. Increasing the cone angle affects the pressure-index curve not only by increasing the surface slope just downstream of the nose, but also by moving the circle of tangency between the cone and the hemisphere forward toward the pressure-measuring orifices. Both aspects of increasing cone angle would contribute to a downstream movement of the sonic line and would cause the orifices to sense a local flow of lower Mach number. The decreasing influence of cone angle as supersonic Mach number increases, the availability of extensive data for hemisphere-cylinders (for example, refs. 1 to 6), and the excellent results obtained with modified Newtonian theory (refs. 7 and 11 to 13) indicate that explicit experimental evaluation of the pressure index for the Ranger vehicle at the higher supersonic and hypersonic Mach numbers is probably unnecessary.

Effect of Reynolds Number on the Pressure Index

The Reynolds numbers for the flow over the hemispherical nose may be important not only because of their influence on model-prototype scaling as such, but also because the Reynolds numbers of both model and prototype vary with Mach number. Reynolds numbers for the present investigation in the Langley 26-inch transonic blowdown tunnel are shown in figure 6. Over the Mach number range covered by these data, Reynolds numbers for the Ranger IV flight were higher than the highest values shown in figure 6 (for total pressure of 70 lb/sq in.) by a factor of 3.3 to 4.3. Although this difference may appear to be large, it is not considered to affect materially the usefulness of the present data because the Reynolds number variations indicated in figure 6, particularly near $M = 0.8$, are shown in figure 4 to have negligible effect on the pressure index. Similar tests on a hemisphere-cone with 10° half-angle in a roughly comparable Reynolds number range also indicated no noticeable effect of varying Reynolds number. This demonstrated insensitivity to Reynolds number in the range of the present tests affords some confidence in the use of present results in connection with the flight of the Ranger IV vehicle. In view of the negligible effect of Reynolds number, most of the present tests were run at a total pressure of 50 lb/sq in. as a compromise between a high Reynolds number and a reasonable running time for the tunnel.

---

[1]The curve for the hemisphere-cylinder represents a compilation made by Henry G. Reichle, Jr. (presently of the Langley Research Center) while he was employed at the George C. Marshall Research Center. This compilation consists of data from references 1 to 6, together with additional data from the Langley Unitary Plan wind tunnel, the Langley 8-foot transonic pressure tunnel, and the Wright Air Development Center, U.S. Air Force.

Effect of Yaw Angle on the Pressure Index

As previously indicated, $|\theta_s|_{max} \leq 10^\circ$ for all the tests, and $|\theta| = |\psi|$ for the tests with $\varphi = 45^\circ$, 135°, and 315°. Thus, for the latter tests equations (1) and (2) give $|\theta|_{max} = |\psi|_{max} = 7.11^\circ$. The inclusion of this amount of yaw had no noticeable effect on the linearity of the curves of $\frac{\Delta p}{q}$ as a function of θ nor on the slopes of these curves. Figure 7 shows that the pressure index is unaffected by this introduction of yaw. Some similar tests of a hemisphere-cylinder (ref. 2) gave similar results for moderately small deflection angles ($\theta < 10^\circ$). Results for a hemisphere-cone with 10° half-angle have indicated that for moderately small yaw angles ψ, the effect of yaw on the curves of $\frac{\Delta p}{q}$ as a function of θ appears to be roughly proportional to $1 - \cos \psi$. For the present tests this quantity is less than 1 percent and hence lies within the scatter of the data.

Effects of Tunnel-Flow Angularity and Model Asymmetry

Figure 3 shows that, in general, $\theta \neq 0$ when $\frac{\Delta p}{q} = 0$. For all the tests, the pitch angle θ for which $\frac{\Delta p}{q} = 0$ (null angle) ranged from 0 to 0.90°. Moreover, the angle generally decreased with increases in either Mach number or total pressure. These nonzero null angles are attributed primarily to tunnel-flow angularity because any effects of model asymmetry would not be expected to vary appreciably with flow conditions. Moreover, when the model is inverted, model asymmetry would tend to reverse the sign of the null angle, whereas flow angularity would tend to maintain the same null angle. (See fig. 8.) The sketches of figure 8 show that the change of null angle with model inversion should give some indication of any significant model asymmetry that may exist. For this investigation such changes of null angle were always less than 0.30°; thus, the effects of model asymmetry appear to be relatively small. Some quantitative aspects of inaccurate orifice location are discussed in appendix I of reference 2. As would be expected figure 4 shows that the presence of flow angularity or slight model asymmetry leads to no significant change in the pressure index when the model is inverted.

CONCLUSIONS

A wind-tunnel investigation has been conducted at Mach numbers from 0.58 to 1.31 to examine some of the characteristics of a differential-pressure system used to measure flow angles over the hemisphere-cone nose of the Ranger IV vehicle. The results lead to the following conclusions:

1. For a given total pressure and Mach number, the differential pressure (measured in the pitch plane) varies linearly with pitch angle at least over the range from -9° to 9°.

2. As Mach number increases above 1, the afterbody shape (downstream of the hemispherical nose) has a decreasing effect on the differential-pressure characteristics, and the present results tend toward those for the hemisphere-cylinder.

3. Within the scope of this investigation, variations in Reynolds number and the introduction of yaw angles up to 7° do not affect the differential-pressure characteristics.

Langley Research Center,
National Aeronautics and Space Administration,
Langley Station, Hampton, Va., June 27, 1963.

REFERENCES

1. Gracey, William: Summary of Methods of Measuring Angle of Attack on Aircraft. NACA TN 4351, 1958.

2. Beecham, L. J., and Collins, S. J.: Static and Dynamic Response of a Design of Differential Pressure Yawmeter at Supersonic Speeds. CP No. 414, British A.R.C., 1958.

3. Beecham, L. J.: The Hemispherical, Differential Pressure Yawmeter at Supersonic Speed. R. & M. No. 3237, British A.R.C., 1961.

4. Roberts, B. G.: Static Response of Hemispherical Headed, Differential Pressure Incidencemeter From M = 1.6 to 2.6. Tech. Note HSA 43, Weapons Res. Establishment, Australian Defence Sci. Service, Nov. 1959.

5. Stine, Howard A., and Wanlass, Kent: Theoretical and Experimental Investigation of Aerodynamic-Heating and Isothermal Heat-Transfer Parameters on a Hemispherical Note With Laminar Boundary Layer at Supersonic Mach Numbers. NACA TN 3344, 1954.

6. Stalder, Jackson R., and Nielsen, Helmer V.: Heat Transfer From a Hemisphere-Cylinder Equipped With Flow-Separation Spikes. NACA TN 3287, 1954.

7. Pasiuk, Lionel: Supersonic Aerodynamic Heat Transfer and Pressure Distributions on a Sphere-Cone Model at High Angles of Yaw. NOL TR 62-35, U.S. Naval Ord. Lab. (White Oak, Md.), June 8, 1962.

8. Sinclair, Archibald R., and Robins, A. Warner: A Method for the Determination of Time Lag in Pressure Measuring Systems Incorporating Capillaries. NACA TN 2793, 1952.

9. Unangst, John R., and Jones, George W., Jr.: Some Effects of Sweep and Aspect Ratio on the Transonic Flutter Characteristics of a Series of Thin Cantilever Wings Having a Taper Ratio of 0.6. NASA TN D-1594, 1963. (Supersedes NACA RM L55I13a and NACA RM L53G10a.)

10. Unangst, John R.: Transonic Flutter Characteristics of a 45° Sweptback Wing With Various Distributions of Ballast Along the Leading Edge. NASA TM X-135, 1959.

11. Keener, Earl R.: Angle of Attack and Sideslip From Pressure Measurements on a Fixed Hemispherical Nose. Jour. Aerospace Sci. (Readers' Forum), vol. 29, no. 9, Sept. 1962, pp. 1129-1130.

12. Baer, A. L.: Pressure Distributions on a Hemisphere Cylinder at Supersonic and Hypersonic Mach Numbers. AEDC-TN-61-96 (Contract No. AF 40(600)-800 S/A 24(61-73)), Arnold Eng. Dev. Center, Aug. 1961.

13. Weinstein, Irving: Heat Transfer and Pressure Distributions on a Hemisphere-Cylinder and a Bluff-Afterbody Model in Methane-Air Combustion Products and in Air. NASA TN D-1503, 1962.

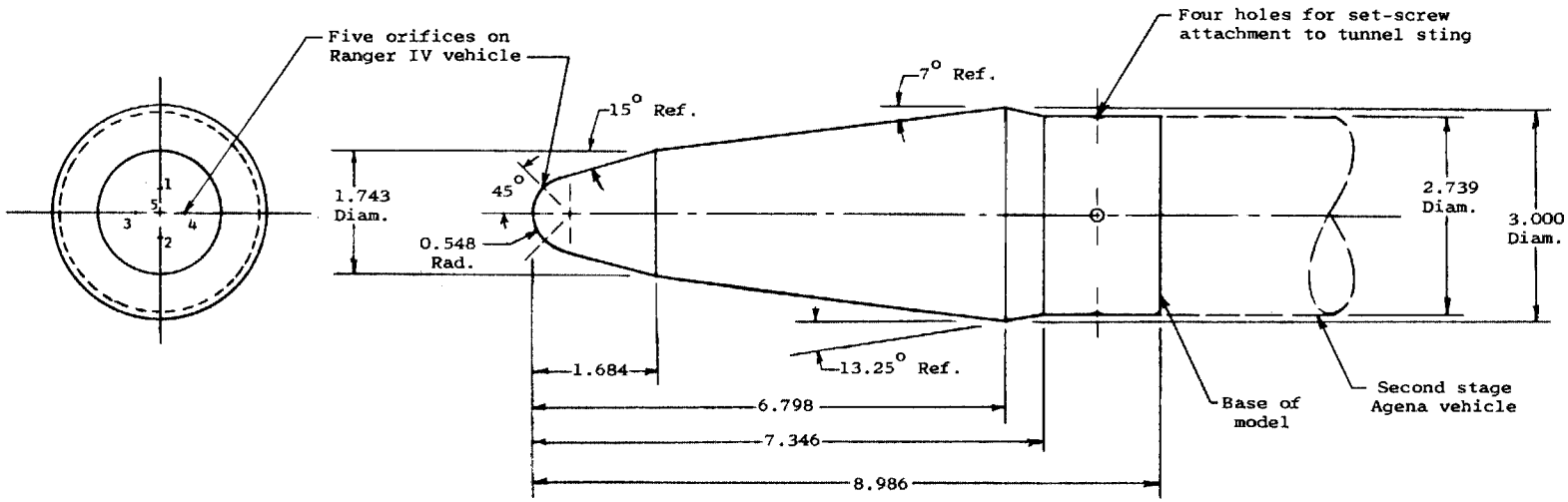

Figure 1.- Sketch of scaled Ranger IV vehicle and of model employed in this investigation. All dimensions are in inches unless otherwise specified. Only orifices 1 and 2 were provided on model.

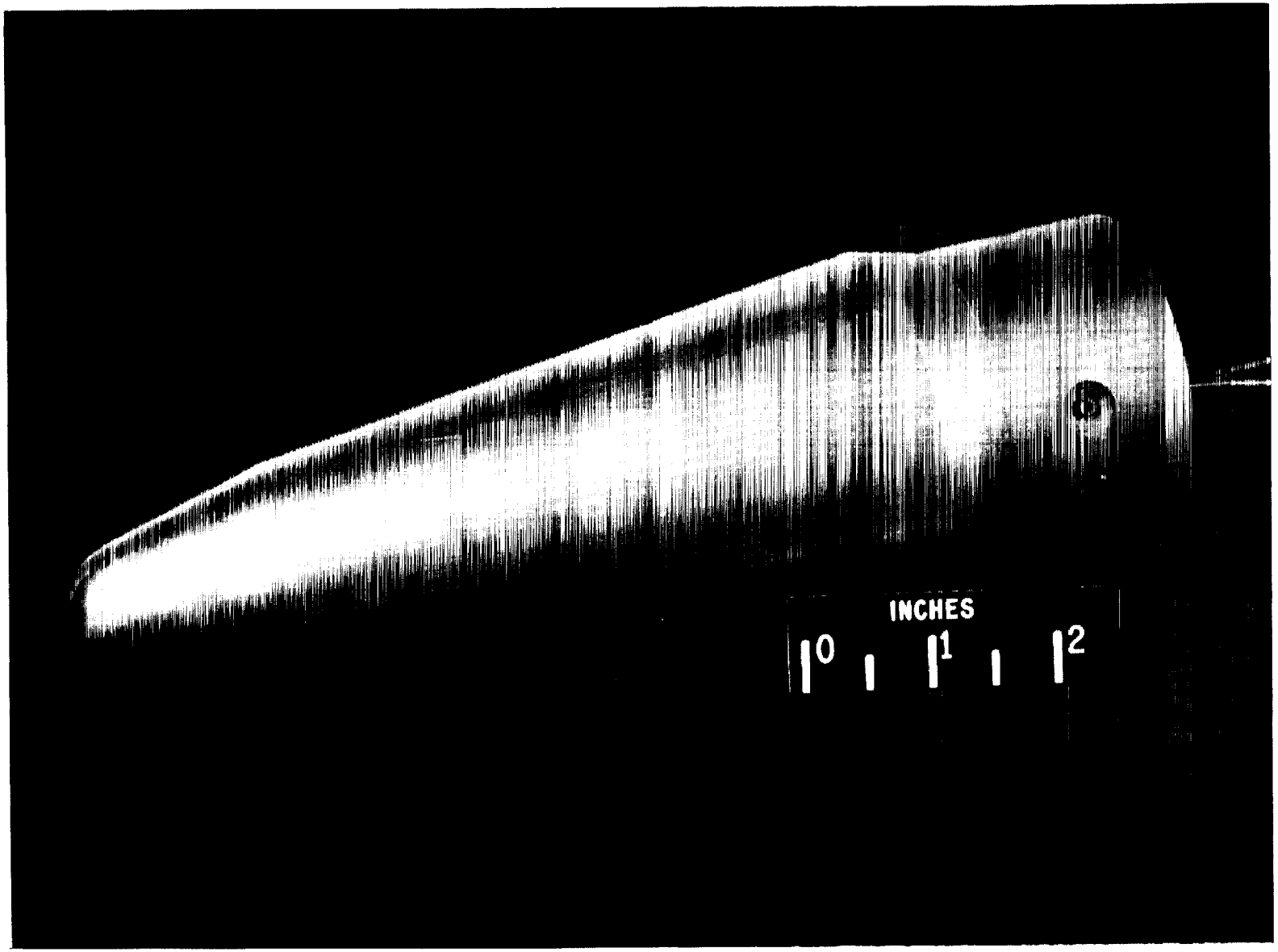

Figure 2.- Photograph of model. L-62-6563

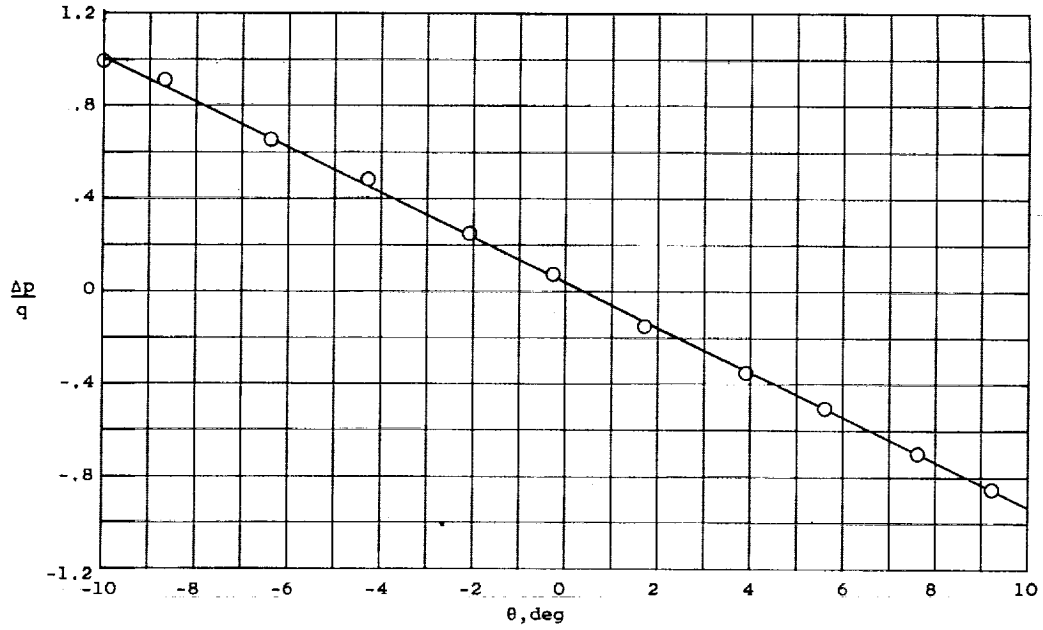

(a) M = 0.585; R = 570,000.

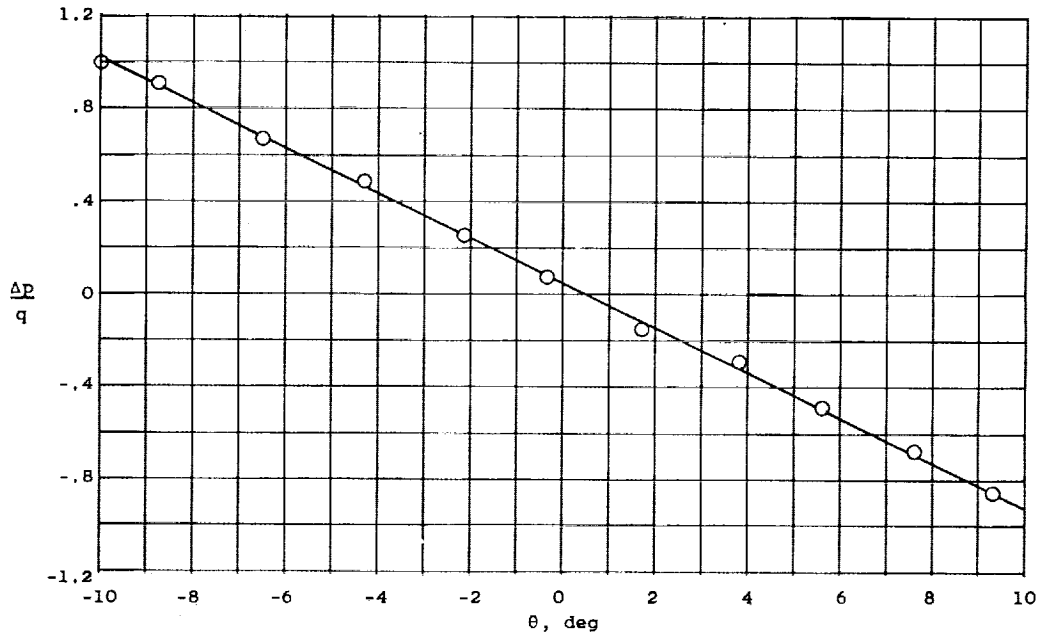

(b) M = 0.815; R = 710,000.

Figure 3.- Relation between differential pressure and geometric pitch angle. $\varphi = 0^{\circ}$; total pressure, 50 pounds per square inch.

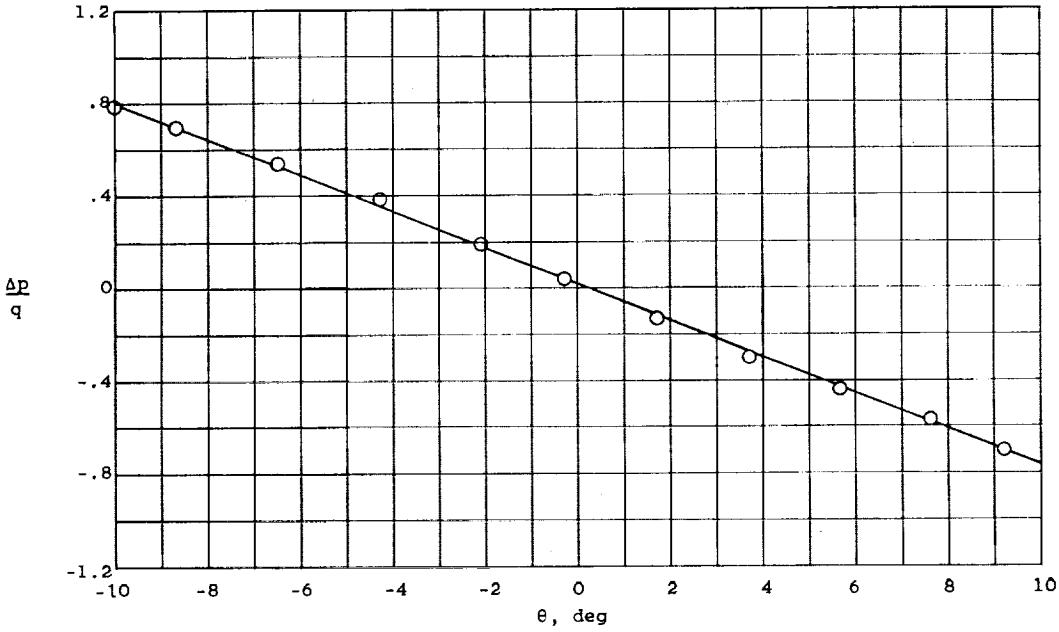

(c) M = 1.049; R = 780,000.

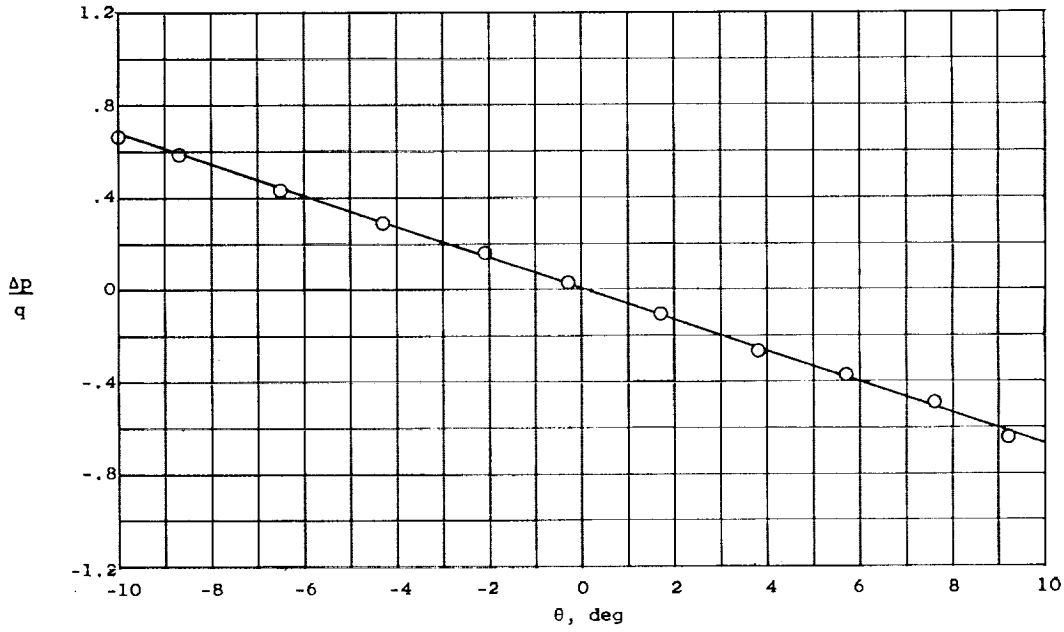

(d) M = 1.310; R = 760,000.

Figure 3.- Concluded.

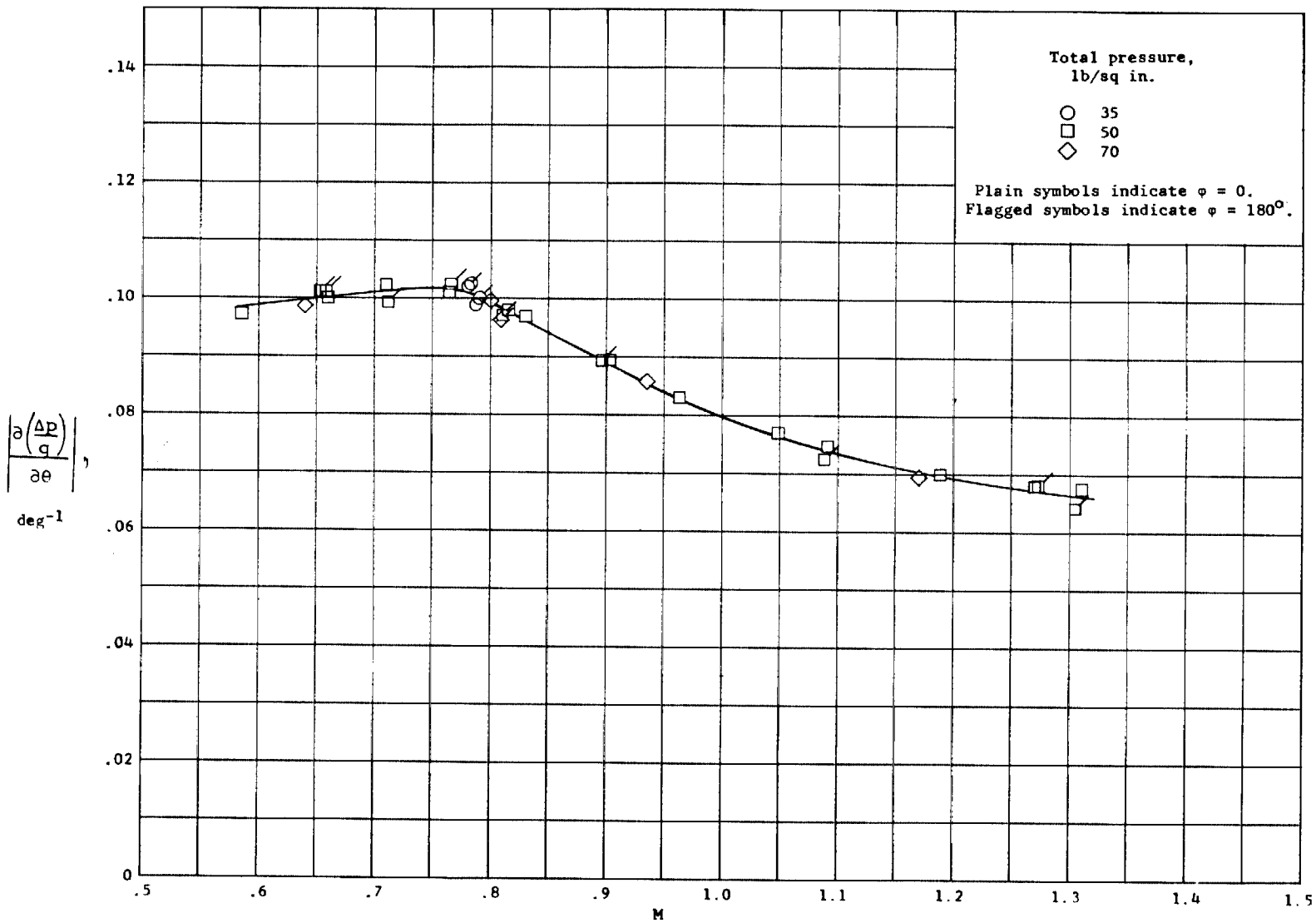

Figure 4.- Variation of pressure index with Mach number.

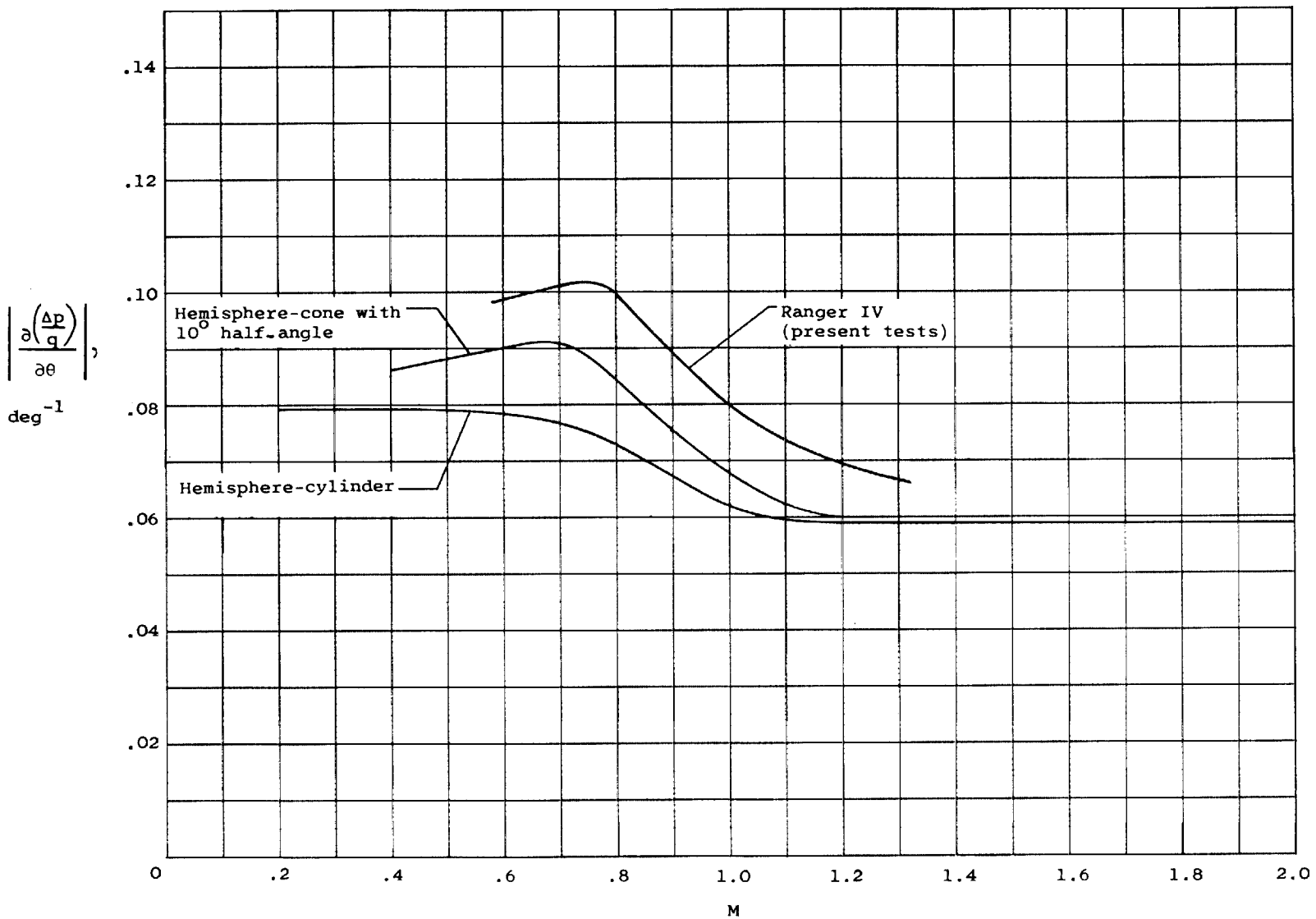

Figure 5.- Comparison of present data for the Ranger IV vehicle with similar results for a hemisphere-cone with 10° half-angle and for the hemisphere-cylinder.

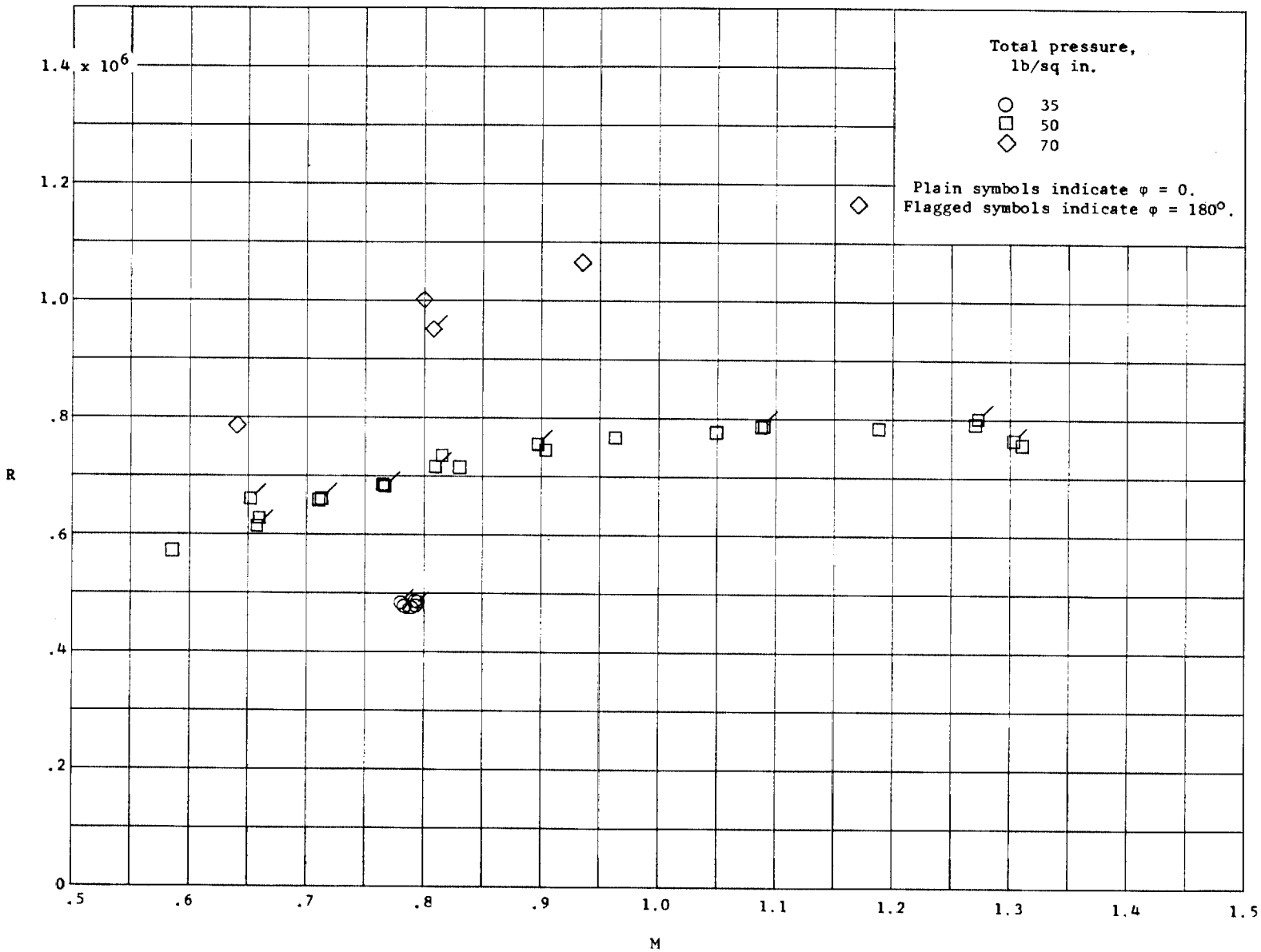

Figure 6.- Variations of Reynolds numbers with Mach number.

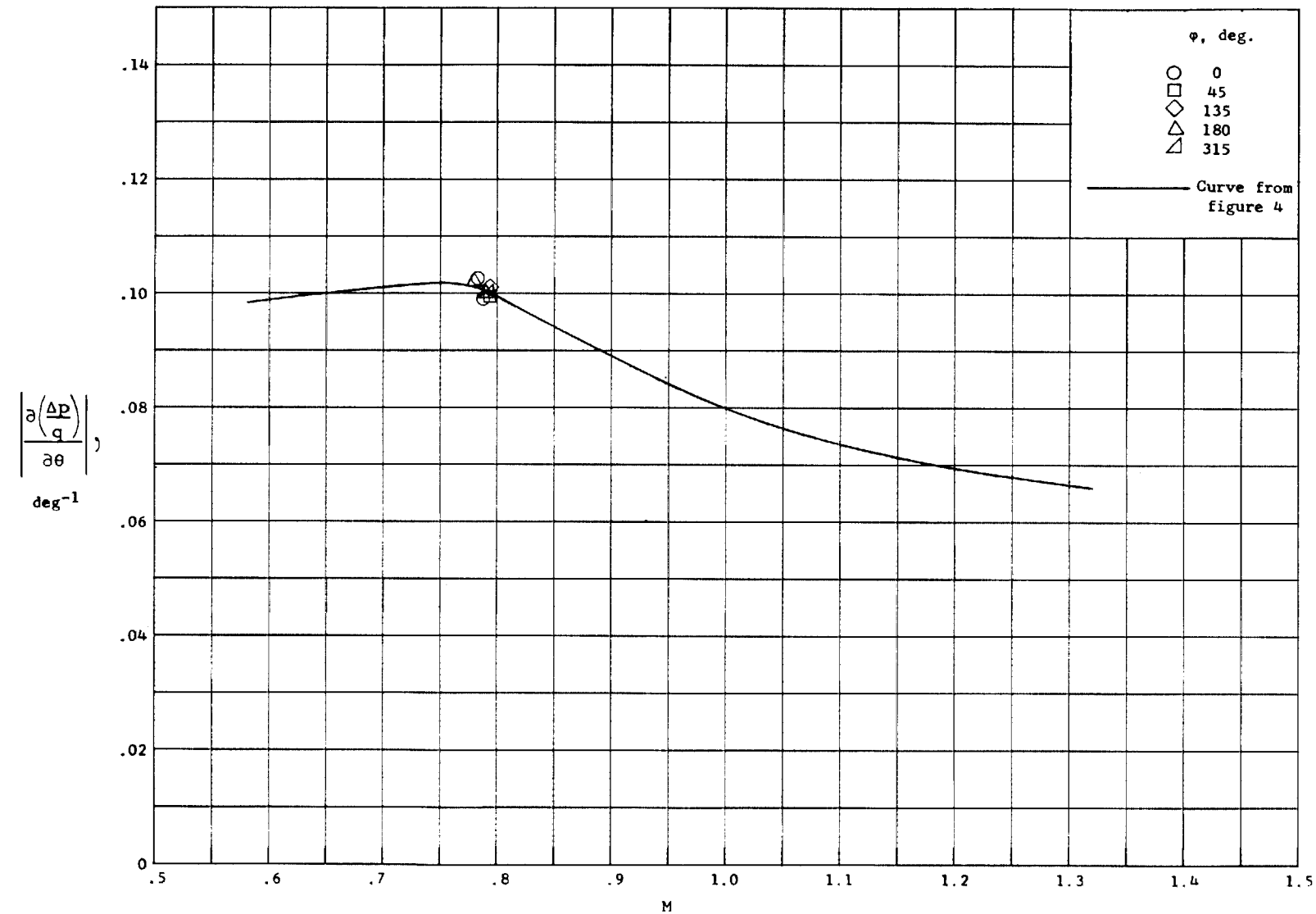

Figure 7.- Effect of roll angle on the pressure index. Total pressure, 35 pounds per square inch.

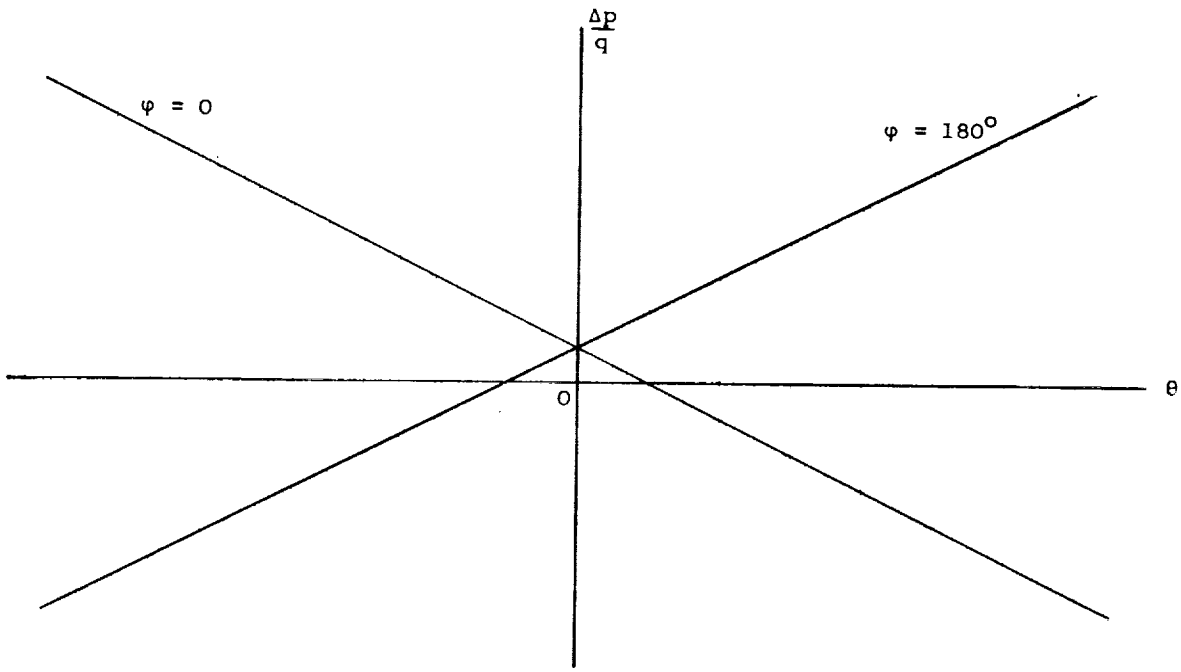

(a) Effect of model asymmetry.

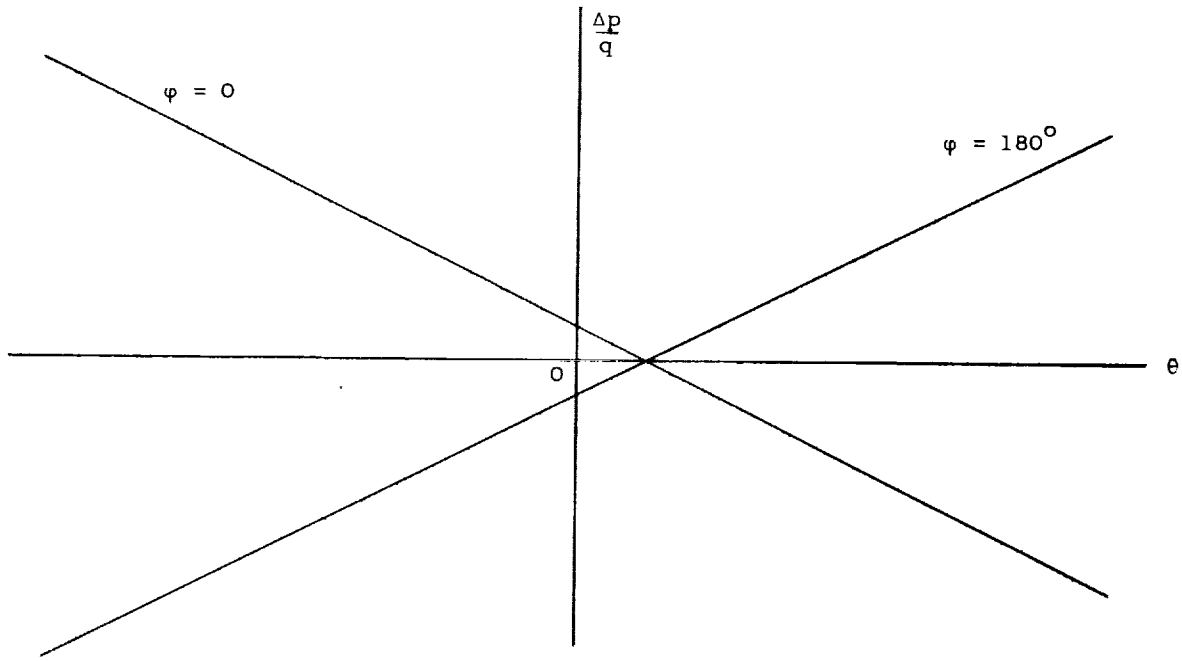

(b) Effect of flow angularity.

Figure 8.- Sketches illustrating effects of model asymmetry and flow angularity at constant Mach number and constant total pressure.

NASA-Langley, 1963 L-3404